Inarticulate past: Incomplete similarity of the ice-climate system and its implications for paleo-records attribution

Mikhail Y. Verbitsky

Gen5 Group, LLC, Newton, MA, USA
UCLouvain, Earth and Life Institute, Louvain-la-Neuve, Belgium
Correspondence: Mikhaïl Verbitsky (verbitskys@gmail.com)

Abstract. Reconstruction and explanation of past climate evolution using proxy records is the essence of paleoclimatology. In this study, we use dimensional analysis of a dynamical model on orbital time-scales to recognize theoretical limits of such forensic inquiries. Specifically, we demonstrate that incomplete similarity does not imply physical similarity and therefore major past events could have been produced by different physical processes making the task of paleo-records attribution to a particular phenomenon to be fundamentally difficult, if not impossible. It also means that any future scenario may not have a unique cause and, in this sense, the orbital time-scale future may be to some extent less sensitive to specific terrestrial circumstances.

Introduction

Interpretation of most prominent events of climate history such as the middle-Pleistocene transition (Ruddiman et al., 1986, Lisiecki and Raymo, 2005, Clark et al., 2021) has been an inspiration for several generations of climate modelers (see for a review Saltzman, 2002, Clark, et al., 2006, Tziperman et al., 2006, Crucifix, 2013, Mitsui and Aihara, 2014, Paillard, 2015, Ashwin and Ditlevsen, 2015, Verbitsky et al, 2018, Willeit et al., 2019, Riechers et al, 2021). While specific physical mechanisms invoked to explain changing glacial rhythmicity vary, they all include slow changes of ocean-atmosphere governing parameters (e.g., Saltzman and Verbitsky, 1993; Raymo, 1997; Paillard and Parrenin, 2004) or glaciation parameters (Clark and Pollard, 1998). On a more general level, all these theories in fact assume slow changes in the intensities of positive (such as, for example, long-term variations in carbon dioxide concentration, e.g., Saltzman and Verbitsky, 1993) or negative (for example, regolith erosion, Clark and Pollard, 1998, or vertical temperature advection in ice sheets, Verbitsky and Crucifix, 2021) system feedbacks. Though all physical phenomena invoked are, indeed, real and may be plausible, the following question still remains unanswered: Is it possible to disambiguate the past and elevate a single "correct" theory? Answering this question is the goal of our study.

Indeed, this is the classical attribution challenge that has been successfully addressed in the context of another well-known problem of geophysics: the causality of the observed global warming. For this purpose, the most comprehensive space-resolving models have been employed to reproduce observed time-series under different conditions and to prove (or discredit) a candidate physical phenomenon (e.g., Stocker, 2014). Certainly, these models cannot be employed on extremely long orbital time-scales (10 – 100 kyr) due to computational constrains. In search for an alternative, we turn here to dimensional analysis. Historically, dimensional analysis and concepts of similarity have been used for studying physical phenomena, complementing even the most sophisticated computational tools and providing physical insight in situations where physical interpretation of the higher-complexity modeling results may be difficult. Here, on orbital timescales, when we retreat from physics-abundant space-resolving models to more conceptual dynamical models, dimensional analysis may be promoted from a supporting to a more prominent role.

Several key terms need to be introduced before we outline the structure of our paper. We will be using the definitions of physical similarity and complete and incomplete similarity as they have been articulated by G. I. Barenblatt (2003). Suppose we have a physical phenomenon that is governed by *n* physical parameters, *k* parameters of which are parameters with independent dimensions. Then, according to the π-theorem (Buckingham, 1914), the phenomenon can be described by *n-k* adimensional similarity parameters $\pi_1, \pi_2, \ldots \pi_i \ldots, \pi_{n-k}$. We will consider two phenomena as being *physically similar* if they are described by identical similarity parameters $\pi_1, \pi_2, \ldots \pi_i \ldots, \pi_{n-k}$. The dimensionless time series of physically similar processes are also identical. If a similarity parameter π_i can be excluded from the description of a physical process (a phenomenon becomes independent of it in the limit that π_i tends to zero or infinity) we can talk about *complete similarity* of this physical process in this parameter: regardless of its specific value, the process does not depend on it. And, finally, we may have *incomplete similarity* when none of similarity parameters $\pi_1, \pi_2, \ldots \pi_i \ldots, \pi_{n-k}$ can be neglected even if they are too small (or too big), but the

53 number of effective parameters may still be reduced because a phenomenon depends not on absolute value of
54 similarity parameters but on their products in some power degree (i.e., conglomerate groups):
55 $\Pi_j = \left(\pi_1^{\alpha_j}\right)\left(\pi_2^{\beta_j}\right)...\left(\pi_i^{\lambda_j}\right)...\left(\pi_{n-k}^{\chi_j}\right)$ $(j = 1,2,...,l; l < n - k)$. Here $\alpha_j, \beta_j, ..., \lambda_j, ..., \chi_j$ are power degrees
56 of $\pi_1, \pi_2, ...\pi_i ..., \pi_{n-k}$ involved into Π_j formulation.
57   We are now ready to proceed with the structure of our paper: (a) first, we will introduce our dynamical
58 model and describe major physical processes involved; (b) using dimensional analysis, we will define 8 similarity
59 parameters $\pi_1 - \pi_8$ that completely define model's behavior; (c) while these adimensional similarity
60 parameters $\pi_1 - \pi_8$ will be determined using simple rules of dimensional analysis, there are no specific algorithms
61 that can help us in finding their effective conglomerate groups Π_j, if they indeed exist. Therefore, we will articulate
62 such conglomerate groups based on observed system behavior; (d) we will then discuss implications of our findings
63 for the attribution challenge and illustrate our reasoning with a numerical experiment; (e) we will conclude our study
64 with some thoughts relating our results to the real-world climate system.
65
66 **Method**
67
68   For our experiments we employ the Verbitsky et al (2018), VCV18 thereafter, dynamical model of the ice-
69 climate system. It has been derived from the scaled mass- and heat-balance equations of the non-Newtonian ice
70 flow, i.e., equations (1) and (2), correspondingly, and combined with an energy-balance equation of the global
71 climate temperature (3):

72 $$\frac{dS}{dt} = \frac{4}{5}\zeta^{-1}S^{3/4}(a - \varepsilon F_S - \kappa\omega - c\theta) \tag{1}$$
73 $$\frac{d\theta}{dt} = \zeta^{-1}S^{-1/4}(a - \varepsilon F_S - \kappa\omega)\{\alpha\omega + \beta[S - S_0] - \theta\} \tag{2}$$
74 $$\frac{d\omega}{dt} = -\gamma[S - S_0] - \frac{\omega}{\tau} \tag{3}$$

75
76   Here, S (m^2) is the area of glaciation, θ (^{o}C) is the basal ice-sheet temperature, and ω (^{o}C) is the global
77 temperature of the ocean-atmosphere (rest of the climate) system. In deriving equations (1) and (2) we considered
78 ice sheets in the thin-boundary-layer approximation such that their inertial forces are negligible relative to stress
79 gradients, and motion equations with very high accuracy can be written in a quasi-static form. For such
80 approximation, a characteristic ice thickness H is connected to ice area S as $H = \zeta S^{1/4}$ where ζ (m$^{1/2}$) is a profile
81 factor assumed to be constant (Verbitsky and Chalikov, 1986, VCV18). Further, equation (1) represents global ice
82 balance $\frac{d(HS)}{dt} = AS$, where, again, $H = \zeta S^{1/4}$ and $A = a - \varepsilon F_S - \kappa\omega - c\theta$ is the surface mass influx. Equation (2)
83 describes vertical ice temperature advection with a time scale $H/(a - \varepsilon F_S - \kappa\omega)$, and equation (3) is the global
84 energy-balance equation. The parameter a (m s^{-1}) is the snow precipitation rate; F_S is normalized external forcing,
85 specifically, mid-July insolation at 65°N (Berger and Loutre, 1991) of the amplitude ε (m s^{-1}) such that εF_S describes
86 ice ablation rate due to astronomical forcing; $\kappa\omega$ is the ice ablation rate representing the cumulative effect of the
87 global climate on ice-sheet mass balance; $c\theta$ represents ice discharge due to ice-sheet basal sliding; $\alpha\omega$ is basal
88 temperature response to global climate temperature change, $\beta[S - S_0]$ is basal temperature reaction to the changes
89 of ice geometry; $-\gamma[S - S_0]$ describes global temperature response to ice geometry changes (e.g., albedo); κ (m s^{-1}
90 ^{o}C^{-1}), c (m s^{-1} ^{o}C^{-1}), α (adimensional), β (^{o}C m^{-2}) and γ (^{o}C m^{-2} s^{-1}) are sensitivity coefficients; S_0 (m^2) is a reference
91 glaciation area; and τ (s) is the timescale for ω. When orbitally forced, the model reproduced events of the last
92 million years reasonably well, except for the interglacial of 400 kyr ago (marine isotopic stage 11). The timing of all
93 other interglacials coincides with Past Interglacial Working Group of PAGES (2016) data (VCV18).
94   We will now focus on the most remarkable feature of the historical records - a period P of climate response
95 to the astronomical forcing. Indeed, it is the change of the climate variability from the predominant period $P = 40$
96 kyr to the main periods of $P = 80-120$ kyr that makes the middle-Pleistocene transition so extraordinary. Though the
97 amplitude increase was considered, until recently, to be a necessary attribute of this transition, its presence in the
98 paleo-records is now questioned (Clark et al, 2021). We begin with the dimensional analysis of the VCV18 system
99 (1) – (3). Indeed, it has 11 governing parameters (including the amplitude ε and the period T of the external forcing).
100 If we choose ε, T and γ to be parameters with independent dimensions, then in accordance with π-theorem a period
101 of the system response can be fully described by 8 dimensionless similarity parameters $\pi_1 - \pi_8$:
102

103    $\pi_1 = \frac{\varepsilon}{a}, \pi_2 = \alpha, \pi_3 = \kappa\gamma\varepsilon T^3, \pi_4 = c\gamma\varepsilon T^3, \pi_5 = \frac{T}{\tau}, \pi_6 = \frac{\gamma T}{\beta}, \pi_7 = \frac{S_0}{\varepsilon^2 T^2}, \pi_8 = \frac{\varsigma}{\varepsilon^{1/2} T^{1/2}},$ and

104

105    $P = T\Psi(\pi_1, \pi_2, \ldots, \pi_8)$ (4)

106

107 At the same time, we observed earlier (Verbitsky and Crucifix, 2020) that the period of the system (1) – (3) response
108 to the obliquity forcing of period T is mostly governed by two dimensionless parameters: by the ratio of the
109 astronomical forcing amplitude to terrestrial ice sheet snow precipitation rate, ε/a, and by the adimensional V-
110 number. The physical meaning of the V-number in the orbital domain becomes most evident if we take a closer look
111 into the structure of positive and negative feedbacks as they appear in the system (1) – (3). The time-dependent
112 negative feedback is proportional to the ice sheet area size as $\beta(S - S_0)$. The coefficient β is defined by
113 thermodynamical properties of an ice sheet, most importantly by the Peclet number, $Pe = \hat{A}H/k$, $\hat{A}$ is a
114 characteristic mass influx, i.e., accumulation minus ablation and k is ice temperature diffusivity (VCV18, Verbitsky
115 and Crucifix, 2021). This negative feedback acts on ice-sheet mass balance with a vertical-advection time delay and
116 is amplified by a sensitivity coefficient c that reflects the intensity of basal sliding. The time-dependent positive
117 feedback is global temperature ω. In the orbital domain, $\tau \ll T$ ($\pi_5 \gg 1$), ω is approximately proportional
118 to $-\gamma\tau(S - S_0)$. The global temperature acts on the ice-sheet mass balance "instantly" as $\kappa\omega$ and with the vertical-
119 advection time-delay as a component of basal temperature conditions, $\alpha\omega c$. Thus, the V-number is emerging in the
120 orbital domain as a ratio of amplitudes of time-dependent positive and negative feedbacks.

121

122    $V = \frac{\gamma\tau}{\beta c}(\alpha c + \kappa)$ (5)

123

124 Specifically, when $V \sim 0.75$ and $\varepsilon/a \sim 1$, the system exhibits the obliquity-period doubling. When the positive
125 feedback and the obliquity forcing are less articulated, the system responds with the 40-kyr period. Thus, slow
126 changes of the V-number (for example, from $V = 0.5$ at $t = 3{,}000$ kyr ago to $V = 0.75$ at $t = 0$) and of the ε/a ratio (for
127 example, from $\varepsilon/a = 0.3$ to $\varepsilon/a = 1.7$ over the same time span) produce a change in the ice-climate behavior similar
128 to the middle-Pleistocene transition.
129 We now notice that the V-number can be presented in terms of similarity parameters $\pi_1 - \pi_8$, specifically:

130

131    $V = \frac{\gamma\tau}{\beta c}(\alpha c + \kappa) = \left(\pi_2 + \frac{\pi_3}{\pi_4}\right)\frac{\pi_6}{\pi_5}$ (6)

132

133 We also experimentally established that the period-doubling sustains ($\Psi = 2$) if, under fixed ε/a and V, the period
134 of the external forcing changes from let say $T = 35$ kyr to $T = 50$ kyr. It can only happen if in this domain similarity

135 parameters π_7 and π_8 make another conglomerate group that does not depend on T, specifically $\frac{\pi_8^4}{\pi_7}$.

136 Thus, equation (4) can be written as:

137

138    $P = T\Psi(\pi_1, \frac{\pi_2\pi_6}{\pi_5}, \frac{\pi_3\pi_6}{\pi_4\pi_5}, \frac{\pi_8^4}{\pi_7}),$ (7)

139

140 that is the pure case of incomplete similarity as we defined it above. Finally we may notice that $\frac{\pi_8^4}{\pi_7} = \frac{H^4}{S_0^2} \ll 1$ for all

141 large ice sheets (thin-boundary-layer approximation). If we set it to be constant and apply generalized π-theorem
142 (Sonin, 2004) we can re-write equation (7) in a more simple form as

143

144    $P = T\Psi(\frac{\varepsilon}{a}, V)$ (8)

145

146   Recognition of incomplete similarity is important because it provides us with a powerful insight: different
147 combinations of similarity parameters π_i may produce the same V-number, i.e., *physically unsimilar processes*
148 (formed by not identical π_i) *may cause the same outcome*. This observation is critical for our attribution challenge.
149 Certainly, precise disambiguation of historical records is always a difficult task because even two physically similar
150 processes having identical adimensional similarity parameters and demonstrating the same behavior may have been
151 produced by different values of physical parameters involved, unless these parameters are physical constants or well
152 defined. The situation becomes especially challenging when we deal with incomplete similarity because, as we just

153 stated, the same results may be produced by not-identical similarity parameters (physically unsimilar processes).
154 This is the theoretical limit that we aspire to expose.
155   We will now apply our findings to the middle-Pleistocene transition. Since the physical interpretation of the
156 governing parameters incorporated in the conglomerate V-number is very straightforward, we may observe a similar
157 (in terms of the period-P bifurcation) system response to changes of a completely different physical nature. For
158 example, parameter β, as we have discussed above, defines intensity of the negative feedback and is formed as a
159 result of interplay between vertical ice advection, internal friction, and geothermal heat flux (VCV18). Increased
160 Peclet number of the growing ice sheet diminishes the role of the geothermal heat flux and may reduce parameter β
161 thus increasing the V-number. The same period-P bifurcation can also be caused, for example, by slow changes in
162 the parameter γ that defines the intensity of the positive feedback and incorporates effects of the albedo change or
163 other atmospheric feedbacks. We solve equations (1) – (3) for two cases we have just described. In both cases we
164 invoke a global cooling trend. In our first experiment (Fig. 1a), this trend is translated into reduction of β, i.e.,
165 weakening of the ice sheet negative feedback, and corresponding increase of the V-number from $V = 0.5$ to $V = 0.75$.
166 We assume here that in growing ice sheets the role of the geothermal heat flux is diminished. The increased
167 continentality of the climate (reduced intensity of the snowfall during colder climate) is accounted by the ε/a ratio
168 increase from $\varepsilon/a = 0.3$ to $\varepsilon/a = 1.7$. In the second experiment (Fig. 1b), the V-number also evolves from $V = 0.5$ to V
169 $= 0.75$, but this time it is achieved by increased intensity of the positive feedback (γ). The millennial forcing is added
170 to εF_S as a single sinusoid of 5 kyr period and doubled (2ε) amplitude. In both experiments, we used mid-July
171 insolation at 65°N (Berger and Loutre, 1991) for the last 3 million years as an astronomical forcing. It is important
172 to note that in the first experiment (changing a and β) only similarity parameters π_1 and π_6 are being changed, but in
173 the second experiment (changing a and γ) the same changes of the V-number are caused by changing $\pi_1, \pi_3, \pi_4, \pi_6$.
174 It means that the processes involved in these two experiments are not physically similar. Though the time-series
175 produced in these two cases are obviously non-identical (see Fig. 1 inserts), we can observe that different physical
176 phenomena may produce the same changes in the conglomerate V-number and the same large-scale effect, i.e., the
177 period-doubling bifurcation at about 1 Myr ago.
178   We do not attempt here to fully reproduce paleo-records such as the Lisiecki and Raymo (2005) or Clark et al.
179 (2021), and a discussion of whether a period doubling should be accompanied by the amplitude increase is outside
180 of the current paper's scope. We will just remark that the amplitude of the system response is the function of not just
181 the period P but also of the ε/a ratio (Verbitsky and Crucifix, 2020) and, for example, less articulated continentality
182 of colder climates may explain diminished amplitude contrasts as it has been recently advocated by Clark et al
183 (2021).
184   Indeed, as we have already indicated, we used mid-July insolation at 65°N (Berger and Loutre, 1991) for the
185 last 3 million years as an astronomical forcing. Apart from that, these examples may also serve as an illustration of
186 some future scenarios of the climate system behavior under post-industrial atmospheric carbon dioxide
187 concentration reduction as implied by Ridgwell and Hargreaves (2007). Again, regardless of the physical nature of
188 the underlying dynamical system, it exhibits 40-kyr rhythmicity of the first 1.5 million years of its evolution and
189 consequent obliquity-period doubling. This probable renaissance of ice-ages is different from the one envisioned by
190 Talento and Ganapolski (2021) which is based on the model tuned to the late Pleistocene (last 800 kyr) ice-volume
191 data and thus postulates only 100-kyr-period variability for the future.
192
193 **Conclusions**

194   The idea of the current presentation is simple but its implication may be important: If ice-climate system has a
195 property of incomplete similarity, then we may be limited in our ability to disambiguate historical records and
196 different physical processes may produce same future scenarios. The latter is intriguing because since B. Saltzman
197 (1962) and E. Lorenz (1963) had discovered a hydrodynamic system's sensitivity to initial conditions, the concept of
198 deterministic chaos became a dominant concept of weather and climate theory. Our findings suggest that if we
199 consider orbital time scales and, instead of time series, focus on their more generalized attributes such as the period
200 of the system response to the astronomical forcing, we may observe that the behavior of these attributes may be, to
201 some extent, less sensitive to the physical nature of the terrestrial governing processes.
202   But is incomplete similarity of the global, orbital-scale, climate system real? So far, this property has been
203 found only in our VCV18 low-order dynamical model, and although this model has been explicitly derived from the
204 conservation laws, the incomplete similarity of the ice-climate system will remain hypothetical until it is supported
205 by empirical data. We speculate, though, that existing historical records may provide some support to this concept.
206 To evaluate the feasibility of a diagnostic approach, let us entertain a simple scaling exercise. Suppose that an
207 empirical time series, such as $\delta^{18}O$ record, is created by a parent system (other than the VCV18) which is controlled

by n physical parameters (k of them having independent dimensions). If we choose the period of the astronomical forcing T to be among parameters with independent dimensions, then in accordance with the π-theorem we have:

$$P = T\Psi(\pi_1, \pi_2, ..., \pi_{n-k}) \tag{9}$$

The wavelet spectrum of the late Pleistocene $\delta^{18}O$ variability in response to the precession (~20-kyr period) and obliquity (~40-kyr period) forcing shows the dominance of 40-kyr and 80-kyr periods (Fig. 1c). If we are willing to accept it as a hint of $\Psi = 2$ for $T = 20$ kyr and for $T = 40$ kyr, then, since some of the similarity parameters $\pi_1, \pi_2, ..., \pi_{n-k}$ depend on T, the period-T independence of Ψ may only happen when $\pi_1, \pi_2, ..., \pi_{n-k}$ make conglomerate T-independent groups. In other words, *period independence of the Ψ function may be a signature of climate system incomplete similarity*. Indeed, the diagnostics of the Ψ function may require much more sophisticated instruments than our *ad hoc* reasoning, and the records will likely not explicitly reveal what the conglomerate similarity groups look like; nevertheless, their mere existence would corroborate the idea of this paper.

Competing interests: The author declares that he has no conflict of interest.

Acknowledgements: The author is grateful to Michel Crucifix for multiple discussions related to this topic and to two anonymous reviewers for their helpful comments.

References

Ashwin, P. and Ditlevsen, P.: The middle Pleistocene transition as a generic bifurcation on a slow manifold, Clim. Dynam., 45, 2683–2695, https://doi.org/10.1007/s00382-015-2501-9, 2015.

Barenblatt, G. I.: Scaling, Cambridge University Press, Cambridge, 2003.

Berger, A. and Loutre, M. F.: Insolation values for the climate of the last 10 million years, Quaternary Sci. Rev., 10, 297–317, 1991.

Buckingham, E.: On physically similar systems; illustrations of the use of dimensional equations, Phys. Rev., 4, 345–376, 1914.

Clark, P. U. and Pollard, D.: Origin of the middle Pleistocene transition by ice sheet erosion of regolith, Paleoceanography, 13, 1–9, 1998.

Clark, P. U., Archer, D., Pollard, D., Blum, J. D., Rial, J. A., Brovkin, V., Mix, A. C., Pisias, N. G., and Roy, M.: The middle Pleistocene transition: characteristics, mechanisms, and implications for long-term changes in atmospheric pCO2, Quaternary Sci. Rev., 25, 3150–3184, 2006.

Clark, P. U., Shakun, J., Rosenthal, Y., Köhler, P., Schrag, D., Pollard, D., Liu, Z., and Bartlein, P.: Requiem for the Regolith Hypothesis: Sea-Level and Temperature Reconstructions Provide a New Template for the Middle Pleistocene Transition. No. EGU21-13981. Copernicus Meetings, 2021.

Crucifix, M.: Why could ice ages be unpredictable?, Clim. Past, 9, 2253–2267, https://doi.org/10.5194/cp-9-2253-2013, 2013.

Lisiecki, L. E. and Raymo, M. E.: A Pliocene-Pleistocene stack of 57 globally distributed benthic $\delta^{18}O$ records, Paleoceanography, 20, PA1003, https://doi.org/10.1029/2004PA001071, 2005.

Lorenz, E.N.: Deterministic nonperiodic flow, Journal of atmospheric sciences, 20, 2, 130-141, 1963.

Mitsui, T. and Aihara, K.: Dynamics between order and chaos in conceptual models of glacial cycles, Clim. Dynam., 42, 3087–3099, 2014.

Paillard, D.: Quaternary glaciations: from observations to theories, Quaternary Sci. Rev., 107, 11–24, https://doi.org/10.1016/j.quascirev.2014.10.002, 2015.

263 Paillard, D. and Parrenin, F.: The Antarctic ice sheet and the triggering of deglaciations, Earth Planet. Sc. Lett., 227,
264 263–271, 2004.
265
266 Past Interglacial Working Group of PAGES: Interglacials of the last 800,000 years, Rev. Geophys., 54, 162–219,
267 2016.
268
269 Raymo, M.: The timing of major climate terminations, Paleoceanography, 12, 577–585,
270 https://doi.org/10.1029/97PA01169, 1997.
271
272 Ridgwell, A., and Hargreaves, J. C.: Regulation of atmospheric CO2 by deep-sea sediments in an Earth system
273 model. Global Biogeochemical Cycles 21, no. 2, https://doi.org/10.1029/2006GB002764, 2007.
274
275 Riechers, K., Mitsui, T., Boers, N., and Ghil, M.: Orbital Insolation Variations, Intrinsic Climate Variability, and
276 Quaternary Glaciations, Clim. Past Discuss. [preprint], https://doi.org/10.5194/cp-2021-136, in review, 2021.
277
278 Ruddiman, W. F., Raymo, M., and McIntyre, A.: Matuyama 41,000-year cycles: North Atlantic Ocean and northern
279 hemisphere ice sheets, Earth Planet, Sc, Lett,, 80, 117–129, https://doi.org/10.1016/0012-821X(86)90024-5, 1986.
280
281 Saltzman, B.: Finite amplitude free convection as an initial value problem—I, Journal of atmospheric sciences, 19,
282 4, 329-341, 1962.
283
284 Saltzman, B.: Dynamical paleoclimatology: generalized theory of global climate change, in: Vol. 80, Academic
285 Press, San Diego, CA, 2002.
286
287 Saltzman, B. and Verbitsky, M. Y.: Multiple instabilities and modes of glacial rhythmicity in the Plio-Pleistocene: a
288 general theory of late Cenozoic climatic change, Clim. Dynam., 9, 1–15, 1993.
289
290 Sonin, A. A.: A generalization of the Π-theorem and dimensional analysis, P. Natl. Acad. Sci. USA, 101, 8525–
291 8526, 2004.
292
293 Stocker, T. (Ed.): Climate change 2013: the physical science basis: Working Group I contribution to the Fifth
294 assessment report of the Intergovernmental Panel on Climate Change, Cambridge University Press, Chapter 10:
295 Detection and Attribution of Climate Change: from Global to Regional, 867–952, 2014.
296
297 Talento, S. and Ganopolski, A.: Reduced-complexity model for the impact of anthropogenic CO2 emissions on
298 future glacial cycles, Earth Syst. Dynam., 12, 1275–1293, https://doi.org/10.5194/esd-12-1275-2021, 2021.
299
300 Tziperman, E., Raymo, M. E., Huybers, P., and Wunsch, C.: Consequences of pacing the Pleistocene 100 kyr ice
301 ages by nonlinear phase locking to Milankovitch forcing, Paleoceanography, 21, PA4206,
302 https://doi.org/10.1029/2005PA001241, 2006.
303
304 Verbitsky, M. Y. and Chalikov, D. V.: Modelling of the Glaciers-Ocean-Atmosphere System, Gidrometeoizdat,
305 Leningrad, 1986.
306
307 Verbitsky, M. Y. and Crucifix, M.: π-theorem generalization of the ice-age theory, Earth Syst. Dynam., 11, 281–
308 289, https://doi.org/10.5194/esd-11-281-2020, 2020.
309
310 Verbitsky, M. Y. and Crucifix, M.: ESD Ideas: The Peclet number is a cornerstone of the orbital and millennial
311 Pleistocene variability, Earth Syst. Dynam., 12, 63–67, https://doi.org/10.5194/esd-12-63-2021, 2021.
312
313 Verbitsky, M. Y., Crucifix, M., and Volobuev, D. M.: A theory of Pleistocene glacial rhythmicity, Earth Syst.
314 Dynam., 9, 1025–1043, https://doi.org/10.5194/esd-9-1025-2018, 2018.
315
316 Willeit, M., Ganopolski, A., Calov, A., and Brovkin, V.: Mid-Pleistocene transition in glacial cycles explained by
317 declining CO_2 and regolith removal, Science Advances 5, 4, https://www.science.org/doi/10.1126/sciadv.aav7337,
318 2019
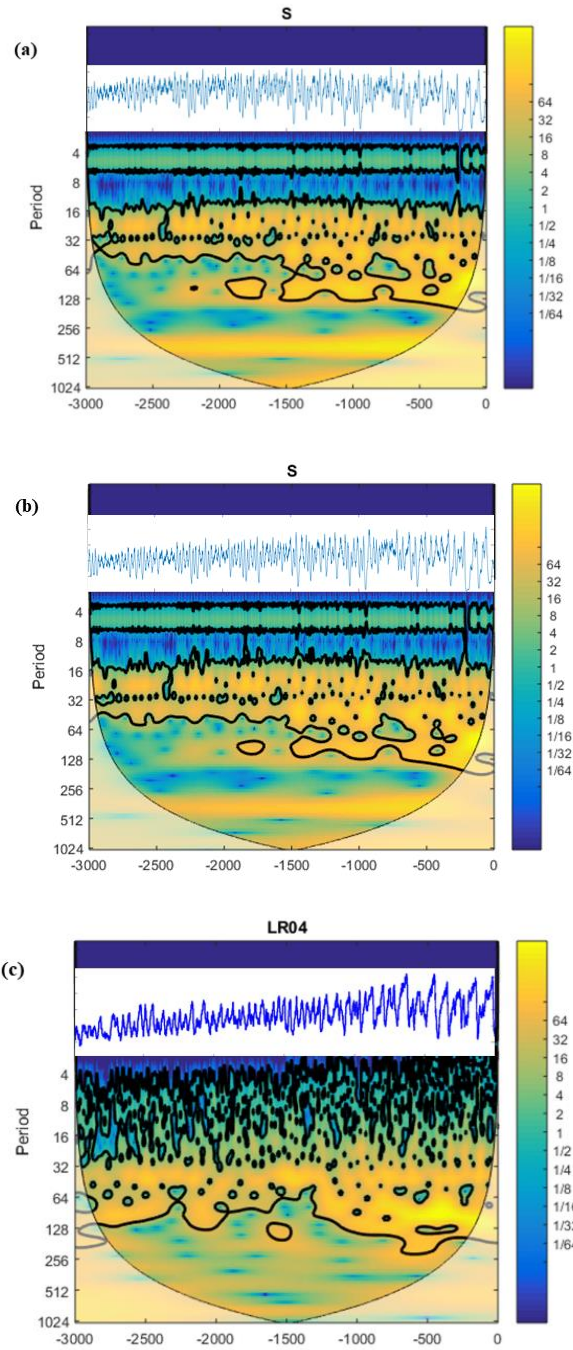
319   **Fig. 1** Ice-climate system response to a cooling trend presented as an evolution of wavelet spectra over 3 Myr for
320   calculated ice-sheet glaciation area S (10^6 km^2) – panels (a) and (b), and for the Lisiecki and Raymo (2005) benthic
321   δ^{18}O record, panel (c). The V-number evolves from $V = 0.5$ to $V = 0.75$ due to weakening of the negative feedback
322   (a) and due to intensified positive feedback (b). The vertical axis is the period (kyr), the horizontal axis is time (kyr
323   before present). The color scale shows the continuous Morlet wavelet amplitude, the thick line indicates the peaks
324   with 95 % confidence, and the shaded area indicates the cone of influence for wavelet transform. Inserts are
325   corresponding time series.